Variation of large-scale regularity in modulated structures of $Ca_2CoSi_2O_7$ studied by a simulation method

Katsuhiro Kusaka,[a]‡ Kenji Hagiya,[a]* Masaaki Ohmasa[a] and Kazuaki Iishi[b]

[a]Department of Life Science, Himeji Institute of Technology, Koto 3-2-1, Kamigori, Akogun, Hyogo 678-1297, Japan, and [b]Department of Chemistry and Earth Sciences, Yamaguchi University, Yoshida, Yamaguchi 753-8512, Japan

‡ Present address: Institute of Materials Structure Science, High Energy Accelerator Research Organization (KEK), Oho 1-1, Tsukuba 305-0801, Japan.

Correspondence e-mail:
hagiya@sci-u.hyogo.ac.jp

The period of two-dimensional modulation in $Ca_2CoSi_2O_7$ varies with temperature (q = 0.285–1/3). The change in the modulated structure with the variation of q has been clarified by the construction of the structures using various q values and the modulation amplitudes determined at 293 K [q = 0.2913 (1), tetragonal]. The features of the modulated structures are characterized by the formation of CaO_6 polyhedra and the variable distribution of bundles along the c-axis, composed of four arrays of CaO_6 polyhedra and an array of CoO_4 tetrahedra. The formation of octagonal arrangements of the bundles is a typical feature of the structures in the incommensurate phase. Large-scale regularities with sizes much larger than the modulation wavelength are also formed in the structures.

1. Introduction

The incommensurate modulation of the structure of synthetic åkermanite ($Ca_2MgSi_2O_7$: a member of the melilite group) and a transition to the non-modulated high-temperature phase were discovered independently by Hemingway *et al.* (1986) and Seifert *et al.* (1987). The latter reported that the modulation wavelength decreases as temperature falls. The modulation wavelength also decreases with an increase in Fe content at the Mg sites. The incommensurate phase was also found in natural melilites (Bindi, Bonazzi *et al.*, 2001; Bindi, Czank *et al.*, 2001).

Hagiya *et al.* (1992, 1993) determined the incommensurate structure in synthetic $Ca_2CoSi_2O_7$ at 293 K by the treatment of X-ray diffraction data in (3 + 2)-dimensional space. The space group is $P_{p4mg}^{P\bar{4}2_1m}$. The structure determination clarified that the Ca—O bond lengths vary widely in the structure and thus the coordination number of Ca varies from six to eight. The variation in the coordination number of Ca was commonly found in the other melilites (Kusaka *et al.*, 1998, 2001; Kusaka, 1999; Bindi, Bonazzi *et al.*, 2001). They also reported that bundles along the c-axis composed of four arrays of the six-coordinated Ca—O polyhedra (CaO_6 array) and a central array of CoO_4 tetrahedra are formed in the structure together with octagonal arrangements of the bundles (to be denoted as 'octagons') as the typical feature of the structure.

The phase transition of incommensurate $Ca_2CoSi_2O_7$ to a low-temperature phase has been described by Riester & Böhm (1997) and Kusaka (1999). Two structures, $P\bar{4}$ (Riester *et al.*, 2000) and $P2_12_12$ (Hagiya *et al.*, 2001), have been reported as the low-temperature phase. Kusaka (1999) indicated that the q value (the magnitude of the primary wavevectors of the modulation waves) varies gradually with temperature changes and the variation is observable in the whole stability range of the incommensurate phase.

research papers

Input data for computation
(i) Atomic coordinates of the independent atoms in the basic structure determined at T_0
(ii) The modulation amplitudes determined at T_0
(iii) The cell parameters of the basic cell
(iv) The symmetry generators in $(3 + 2)$-dimensional space
(v) The q value of the structure at the desired temperature
(vi) The ratio of $|F(T)|/|F(T_0)|$
(vii) The initial phase of the modulation
(viii) The area to be constructed

Process of the computation
(i) Calculations of the coordinates of the atoms in three-dimensional space using eqns (1) and (2) and the symmetry generators
(ii) Evaluation of all Ca—O distances in the area to be drawn
(iii) Drawing of the outlines of the polyhedra (their forms are pentagons) around Ca atoms and plotting of the Ca atoms with dots. The drawing is a projection along the c axis
(iv) Shading of the pentagons corresponding to the six-coordinated Ca—O polyhedra. The criteria assigning these polyhedra are described in the text

The variation of q caused by temperature changes has been observed in many studies, as described above. Investigations into the structure change induced by this phenomenon are very important to clarify the following crystal-chemical problems: how the variation of the structure occurs by a change in q and what the common features in the structures with different q values are. The present studies have consequently been undertaken to clarify these problems by constructing the structures with various q values using the modulation amplitudes of atoms determined at 293 K.

2. Method of the construction of the modulated structures

For the construction of the modulated structures we assumed that the modulation of the structure in the higher-dimensional space stays unchanged through temperature variation, but that a systematic phase change of the modulation waves is induced by the variation of q; that is, the phase change is expressed as the deformation of the $(3 + 2)$-dimensional cell. The assumption is based on the following observations:

(i) no distinct change in the intensity distribution of the satellites in reciprocal space was detected through observations at different temperatures;

(ii) the higher harmonics of the satellite reflections were detected even at low temperature only on X-ray photographs exposed for very long times.

We then developed a computer program (K. Hagiya & K. Kusaka, unpublished) to calculate and plot the three-dimensional coordinates of the atoms in $(3 + 2)$-dimensional space using the following formulae (Hagiya *et al.*, 2001)[1]

---

[1] The same expressions as used in §3 of Hagiya *et al.* (2001) are inappropriate. They should be written with T rather than q, and t_1 and t_2 should be written with their initial phases t_1^0 and t_2^0.

$$\mathbf{x}_j = \mathbf{n} + \bar{\mathbf{x}}_j + \mathbf{u}_j, \qquad (1)$$

where $\mathbf{x}_j$ is the position vector of atom j, $\mathbf{n}$ a lattice vector of the basic cell, $\bar{\mathbf{x}}_j$ a position vector in the unit cell of the basic structure and $\mathbf{u}_j$ is a displacement vector. The magnitudes $u_{ij}(T)$ ($i = 1, 2, 3$ corresponding to x, y, z) at temperature T are given as

$$u_{ij}(T) \simeq [|F(T)|/|F(T_0)|] \sum_m \sum_n [A_{ij}^{mn}(T_0) \cos 2\pi(mt_1 + nt_2)$$
$$+ B_{ij}^{mn}(T_0) \sin 2\pi(mt_1 + nt_2)], \qquad (2)$$

where $A_{ij}^{mn}(T_0)$ and $B_{ij}^{mn}(T_0)$ are Fourier amplitudes of the modulation at T_0 (= 293 K in the present case), and m and n are the indices of the satellite reflections. The parameters t_1 and t_2 are the internal phases of the modulation at the atomic
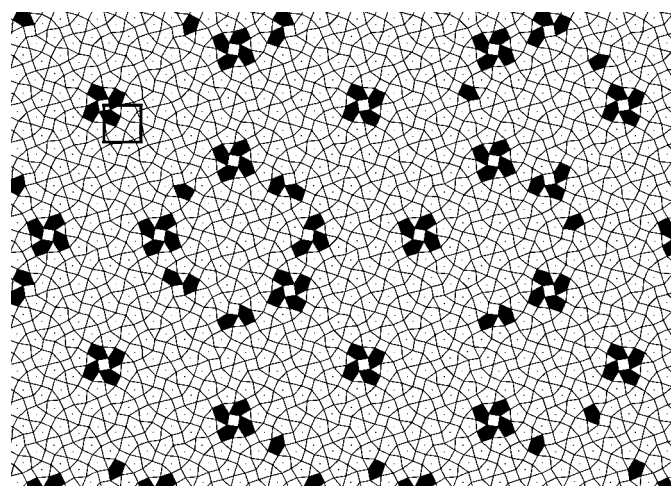
(a)
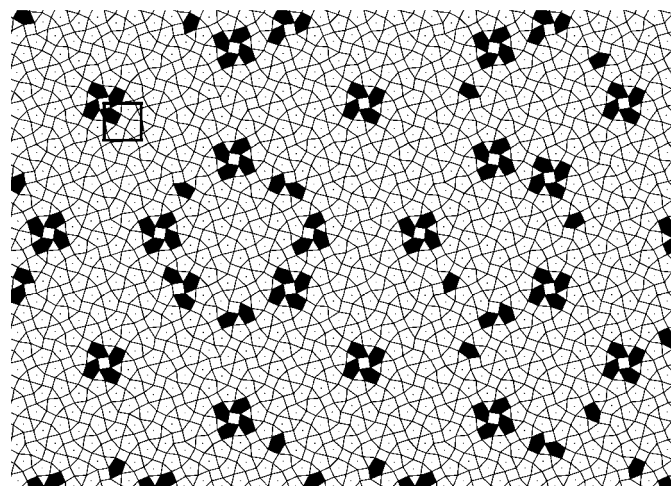
(b)

Figure 1
(a) The incommensurate structure of $Ca_2CoSi_2O_7$ determined at 468 K ($q = 0.289$). (b) The structure constructed with $q = 0.289$ and the amplitudes determined at 293 K. Both structures are constructed with $t_1^0 = 0$ and $t_2^0 = 0$. Triangles denote SiO_4 tetrahedra, squares CoO_4 tetrahedra and pentagons Ca—O polyhedra. Dots indicate Ca sites. Shaded pentagons correspond to the arrays of the CaO_6 polyhedra. The larger square in the upper-left part indicates the basic tetragonal cell [$a = 7.8563$ (4), $c = 5.0294$ (3) Å] with the origin at the $\bar{4}$ axis.

Table 2
Relation between initial phases (t_1^0, t_2^0) and possible space groups of the commensurate structure with $q = N/M$.

Structures with the other arbitrary initial phases have lower symmetry ($P1$). Independent ranges to enumerate CaO$_6$ arrays and bundles are also given.

M	Even			
Cell parameter	$Ma/2^{1/2}$			
t_1^0	$= n_1/M$	$= (2n_1 + 1)/2M$	$= (2n_1 + 1)/2M$	$\neq (2n_1 + 1)/2M$
t_2^0	$= n_2/M$	$= (2n_2 + 1)/2M$	$\neq (2n_2 + 1)/2M$	$= (2n_2 + 1)/2M$
Space group	$P\bar{4}$	$Pba2$	Pa	Pa
Independent ranges	$0 \leq t_1^0 < 1/M$ and $0 \leq t_2^0 < 2/M$			

M	Odd			
Cell parameter	Ma			
$t_1^0 + t_2^0$	$= n_1/M$	$= (2n_1 + 1)/2M$	$= (2n_1 + 1)/2M$	$\neq (2n_1 + 1)/2M$
$-t_1^0 + t_2^0$	$= n_2/M$	$= (2n_2 + 1)/2M$	$\neq (2n_2 + 1)/2M$	$= (2n_2 + 1)/2M$
Space group	$P\bar{4}$	$P2_12_12$	$P2_1$	$P2_1$
Independent ranges	$0 \leq t_1^0 < 1/M$ and $0 \leq t_2^0 < 1/M$			

(n_1, n_2 are integers).

position $\mathbf{n} + \bar{\mathbf{x}}_j$ with the initial phases t_1^0 and t_2^0: $t_1 = \mathbf{k}_1 \cdot (\mathbf{n} + \bar{\mathbf{x}}_j) + t_1^0$ and $t_2 = \mathbf{k}_2 \cdot (\mathbf{n} + \bar{\mathbf{x}}_j) + t_2^0$. $\mathbf{k}_1 = q(\mathbf{a}^* + \mathbf{b}^*)$ and $\mathbf{k}_2 = q(-\mathbf{a}^* + \mathbf{b}^*)$, where $\mathbf{a}^*$ and $\mathbf{b}^*$ are the base vectors of the reciprocal basic cell. The input data for the constructions and the process in the program are briefly listed in Table 1. The applicability of the above formulae was ascertained by the structure analyses at 468 K [$q = 0.289$ (4); Kusaka *et al.*, 2001] and 170 K ($q = 1/3$; Hagiya *et al.*, 2001). Fig. 1 indicates the agreement between the structure determined with the diffraction data at 468 K and that constructed with the above formulae. Since a characteristic feature of the

incommensurate structure is the formation of CaO$_6$ polyhedra (Hagiya *et al.*, 1993), a routine to assign those polyhedra was added in the program by which the CaO$_6$ polyhedra are selected from the rest using threshold distances. The threshold values were determined from the tables of Ca—O distances published by Smyth & Bish (1988).

3. Constructed structures with various q

A total of 101 structures of the incommensurate phase with q values from 0.27 to 0.32 and with intervals of 0.0005 were constructed for the survey of the crystal-chemical features of the modulated structures. The above range covers the observed q values of the material (between 0.285 and 0.310). The area of the construction is a square $100a \times 100a$ ($\simeq 784 \times 784$ Å^2), where a is the length of the a-axis of the basic cell. $|F(T)|/|F(T_0)|$ was fixed to 1. Each of the initial phases t_1^0 and t_2^0 was varied from 0.0 to 0.9 with an increment of 0.1. Many rational numbers ($q = N/M$, with rather small M) are contained in the above range and some of those initial phases do not give the structures which are appropriate to obtain the averaged features: for $q = 3/10$, those initial phases give the same structures. Consequently, the enumeration for four (11/40, 7/25, 23/80 and 3/10) rational q values was made in the independent range indicated in Table 2.

The Ca atoms in the structures of the non-modulated high-temperature phase have a coordination number of eight. The most prominent differences of the structural features in incommensurate and commensurate structures from those in the non-modulated structure are the generation of the CaO$_6$ arrays along the c axis and the formation of the bundles of the CaO$_6$ arrays. Thus, variations in the numbers of CaO$_6$ arrays and bundles were enumerated in the structures with different q values by summing up those numbers in $100a \times 100a$ squares of the structures constructed with 100 different initial phases. Then the total sums are divided by 100, which is the number of different initial phases. The results are depicted in Fig. 2. The values indicated in Fig. 2 are there-
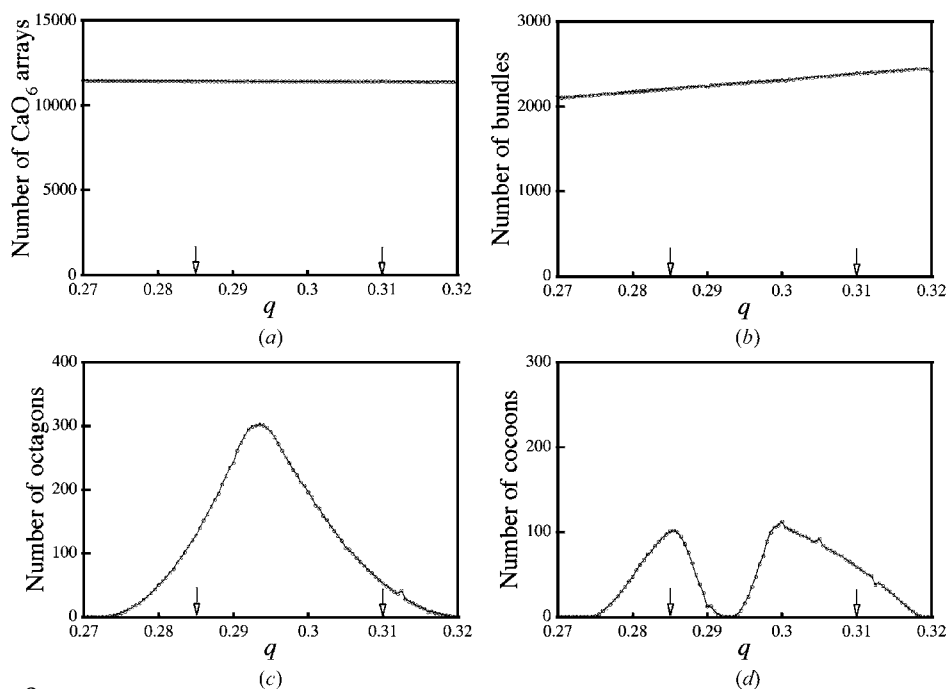
Figure 2
Variation in the numbers of (*a*) CaO$_6$ arrays, (*b*) complete bundles, (*c*) octagons of bundles and (*d*) cocoon patterns *versus* q. The arrows in each diagram indicate the observed range of q. The small irregularities on the curves are caused by errors in the calculation of the average values. The longer axis of the cocoon is parallel to $\langle 100 \rangle$ in the lower q value range and is parallel to $\langle 110 \rangle$ in the higher q range.

fore the average numbers for the 100 different initial phases.

The numbers of the CaO_6 arrays (Fig. 2a) are almost constant in the whole range of the q values and amount to 28% of the total Ca sites in a $100a \times 100a$ square. The numbers of complete bundles composed of four CaO_6 arrays and a central array of CoO_4 tetrahedra were then enumerated. The number of complete bundles increases slightly with an increase in q (Fig. 2b), that is, with a fall in temperature. The numbers of the bundles indicate that 74–86% of the CaO_6 arrays form bundles in the structures. This reveals that most of the CaO_6 arrays are arranged to form bundles and suggests that in the modulated structures there should be a tendency to form bundles. Then variations in the arrangements of bundles were examined in the constructed structures and the common features of the distribution of bundles were also detected. The constructed structures showed that most of the bundles form groups in the modulated structures based on the formation of octagonal arrangements (octagons) with sides $(5/2)^{1/2}a$ ($\simeq$ 12.4 Å, where a is the edge of the tetragonal basic cell) or fragments of the octagons lacking one or more vertices. The most prominent feature in a wide range of q values is the formation of complete octagons of bundles. Fig. 2(c) indicates the numbers of complete octagons versus q values. The numbers are markedly high in the observed q range and very low outside of the range. The curve shows the maximum at $q = 0.2935$. Approximately 83% of the bundles in a $100a \times 100a$ square are related to the formation of octagons at $q = 0.2935$. Some of the fragments are linked and indicate composite patterns (such as a cocoon and other complex forms) in narrow ranges of q values. A cocoon-like arrangement, an interpenetrated form of two incomplete octagons with seven bundles, is one of the typical composite forms of octagons in the observed q range (Fig. 2d). This feature suggests that the formation of the octagons should be the most prominent regularity induced in the incommensurate phase and may have a close relation to the stability of the modulation
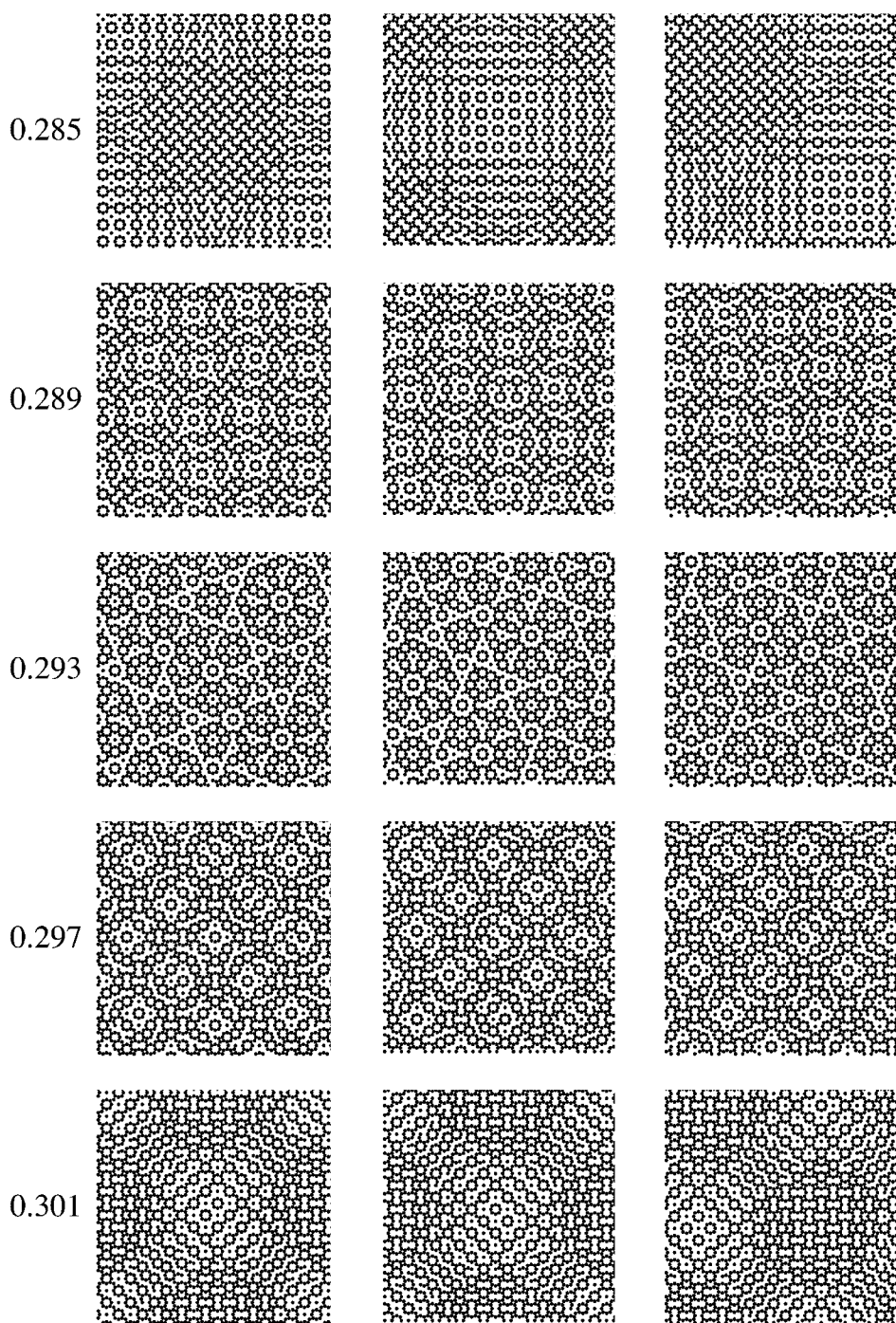

Figure 3
Schematic diagrams of the distribution of the complete bundles in the structures with q values from 0.285 to 0.301. Initial phases (t_1^0, t_2^0) used are $(0, 0)$ for the structures in the first column, $(1/400, 201/400)$ for the second column and $(2^{1/2}/10, 3^{1/2}/10)$ for the third column. The size of the area in each diagram corresponds to $100a \times 100a$.

period, which is incommensurable or commensurable to the periodicity of the cell of the basic structure.

Five sets of diagrams of the structures constructed with different q values and initial phases are depicted in Fig. 3 as examples of incommensurate structures. Only complete bundles are indicated with solid circles and the incomplete bundles are not indicated in order to make the variation in the arrangements clear. The initial phase of each diagram in the first column is (0, 0) and gives $P\bar{4}$ as the space group. The initial phases (t_1^0, t_2^0) selected for the structures in the second column are set close to (0, 1/2) and give the different space group ($Pba2$) from $P\bar{4}$. Each initial phase of the diagrams in the third column is $(2^{1/2}/10, 3^{1/2}/10)$ as an arbitrary one. The constructions of the structures with various q values (0.285–0.301 where $\Delta q = 0.004$) display that the distribution of the octagons of the bundles in the structure changes sensitively with a small deviation of q values (ca 1.4% of the magnitude of q). A non-periodic distribution is generally formed in the structures with irrational q values.[2] At $q = 0.285$, the octagons and cocoons are the main components of the structure. The diagram with $q = 0.301$ consists of the same components as those in the structure at $q = 0.285$. The long axes of cocoons are parallel to $\langle 110 \rangle$ of the basic cell in the former, while they are parallel to $\langle 100 \rangle$ in the latter. Most of the octagons form a wide band structure (almost 350 Å in width) parallel to $\langle 100 \rangle$ in the structure of $q = 0.285$. The similar bands in the structure of $q = 0.301$ are 210 Å in width. The structures with $q = 0.289$ and $q = 0.297$ also have pseudo-periods with almost the same width at ~ 210 Å. Bands consisting of octagons and cocoons form a pseudo-periodic arrangement in each diagram. The directions of the bands are parallel to $\langle 100 \rangle$ in the former and $\langle 110 \rangle$ in the latter. The diagram with $q = 0.293$ shows different features from the other structures and indicates the octagonal arrangements of the octagons. White streaks intersecting each other with angles of integral multiples of 45° are distinct. Regular arrangements of the octagons are formed with rational q values (e.g. $q = 2/7$, 3/10). In the structures with $q = 0.2857$ ($\sim 2/7$) and 0.3 ($= 3/10$), all octagons are distributed at the lattice points of their large tetragonal primitive lattices with almost the same size (the periods of the lattice are ca 55 Å, Fig. 4). The lattice is parallel to $\langle 100 \rangle$ of the basic cell in the structure with $q = 0.2857$, but the lattice is parallel to $\langle 110 \rangle$ in the structure with $q = 0.3$. The structures constructed with the other initial phases (also discussed in §4) show different features from those indicated in Fig. 4. The similarity of both structures and the difference between their orientations can be ascribed to almost the same but opposite deviations from the special q value ($q = 1 - 1/2^{1/2}$), giving the 'regular-octagon' distribution of satellite reflections. These features are derived from the apparent symmetry of their lattices (tetragonal) and the property of the two-dimensional modulation.

The method was also applied to the construction of structures with $q = 1/3$. The transition between the incommensurate

and commensurate phases may be regarded as a change in the structure but keeping their averaged structures unchanged, because the apparent space groups and intensity distributions observed in the main reflections for both phases are the same. This also implies that a commensurate structure may be described in $(3 + 2)$-dimensional space as a variable of the incommensurately modulated structures having a rational q value ($q = 1/3$) and, therefore, the structure of the commensurate phase in three-dimensional space may be constructed by the same method as applied to the incommensurate phase. The commensurate structure (orthorhombic, $P2_12_12$) was determined with the initial parameters derived by the present method (Hagiya et al., 2001). The numbers of CaO_6 polyhedra, bundles and octagons were enumerated in the commensurate structures constructed with various initial phases. The ratio of the number of CaO_6 arrays to the total number of Ca sites in a $3a \times 3a$ square varies from 16.7 to 44.4% and the ratio of the number of CaO_6 arrays forming complete bundles to that of the total CaO_6 arrays changes from 50 to 100%. The commensurate structure ($P2_12_12$) is the structure with maximum values (44.4 and 100%, respectively), while these two values are low in the $P\bar{4}$ structure (22.2 and 50%, respectively). A number of structures with $q = 1/3$ were constructed with other arbitrary initial phases and they show various arrangements of the bundles. Almost all have low symmetry such as $P1$.

4. Discussion

The structure change in $Ca_2CoSi_2O_7$ related to the variation of q (between 0.27 and 0.32, and 1/3) has been clarified by the construction of the structures with their q values and the modulation amplitudes determined at 293 K. The structures are characterized by the distribution of complete bundles formed with four CaO_6 arrays and an array of CoO_4 along the c axis. Many bundles are arranged octagonally (form octagons) in the observed range of q values. Although the
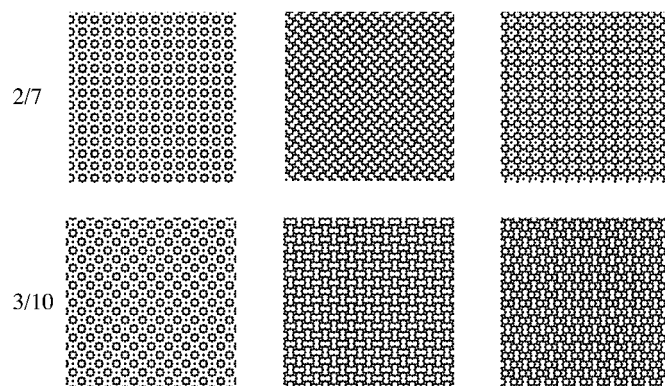

Figure 4
Schematic diagrams of the commensurate structures constructed with $q = 2/7$ and 3/10. Both structures constructed with initial phases (t_1^0, t_2^0) at (0, 0) are indicated in the first column. The initial phases of the second column are (0, 1/2) for $q = 2/7$ and (1/20, 11/20) for $q = 3/10$. Both structures in the third column are constructed with $(2^{1/2}/10, 3^{1/2}/10)$. The size of the area in each diagram corresponds to $100a \times 100a$.

[2] Irrationals cannot be accurately expressed on a digital computer. The q values indicated in Fig. 2 as irrationals are therefore all rational in the strict sense. The constructed structures should reveal the features in the structures with irrational q, because they have very large periods.

formation of octagons is the most remarkable feature in the incommensurate phase, direct imaging of the octagons in $Ca_2CoSi_2O_7$ by HRTEM has not been reported so far. However, Heurck et al. (1992) observed many octagons in the HRTEM images of $Ca_2ZnGe_2O_7$. Fig. 14 of their paper indicates one of the octagons with eight dots. The four bright spots surrounding each dot may be the four arrays of the CaO_6 polyhedra in a bundle. Those octagons probably correspond to the octagonal arrangement of the bundles found in $Ca_2CoSi_2O_7$, although some of the constituent atoms are different. Various large-scale regularities (the octagons, the cocoons, the octagonal arrangements of the octagons and the pseudo-periods) are formed from different arrangements of the bundles, as shown in Fig. 3, and the regularities are sensitive to changes in q values. The sizes of those large-scale regularities are much larger than the modulation wavelengths.

The selection of an initial phase (t_1^0, t_2^0) is very important in the construction of the commensurate structure. Since each parameter of the atoms in the $(3 + 2)$-dimensional space is represented in a repeating unit spanned by the two internal phases t_1 and t_2 [to be denoted as 'the (t_1, t_2) area'], the complete structural information of an incommensurate phase is enclosed in the whole continuous area of the (t_1, t_2) area. However, information about a commensurate structure is given only at specific positions (or phases) in the (t_1, t_2) area owing to the commensurable relation between modulation periods and the basic cell edges. For $q = 1/3$, complete information on the structure is localized at discrete positions in the (t_1, t_2) area separated with one third of the unit lengths of t_1 and t_2. This situation of the commensurate structures with a short period has been discussed by van Smaalen (1987) using examples in the $(3 + 1)$-dimensional space. The discreteness of the structure information indicates that different relations between the origins of the three-dimensional basic cell and the (t_1, t_2) area may generate different structures and these different structures correspond to different intersections of the three-dimensional space in the $(3 + 2)$-dimensional space. However, the incommensurate structures essentially include the whole structures given by different initial phases.

The crystallographic features of the commensurate structures are given in Table 2. The orientations of the cell edges depend on the denominator M from $q = N/M$ and the space groups of the constructed structures depend on the initial phases. The structures with $q = 2/7$ and 3/10 are also commensurate and constructions with different initial phases give different structures. The structure ($q = 2/7$) constructed with the initial phase (0, 1/2) (the second column in Fig. 4) is quite different (orthorhombic) from that indicated in the first column. No octagon of the bundles are formed in it, but cocoon patterns of bundles are formed. The apparent symmetry of each diagram in the second and third columns is high, but the true symmetry of the structure is given in Table 2. The structure with an arbitrary initial phase, $(2^{1/2}/10, 3^{1/2}/10)$, gives a different feature of octagon distribution from that of the first column. The structure constructed with the initial phases (0, 0) and (1/2, 1/2) are in a twin relation, and those

with (1/2, 0) and (0, 1/2) are also in a twin relation. The structures of $q = 3/10$ constructed with the initial phases (0, 0), (1/20, 11/20) and $(2^{1/2}/10, 3^{1/2}/10)$ are also indicated in Fig. 4. The structure of (1/20, 11/20) is again an orthorhombic one. The structures constructed with (0, 0) and (1/2, 1/2), being the same, are in a twin relation to those with (1/2, 0) and (0, 1/2).

The two commensurate structures ($q = 1/3$), $P\bar{4}$ and $P2_12_12$, are constructed with the modulation amplitudes determined at 293 K. The specimens with these two structures were synthesized and the structures were determined (Riester et al., 2000; Hagiya et al., 2001). This fact indicates that the change of the modulated structure of $Ca_2CoSi_2O_7$ with a variation of q can be regarded as the systematic phase change of the modulation waves induced by deformations of the $(3 + 2)$-dimensional cell as assumed in §2. The symmetry of the transformed structure is affected, in that case, by the choice of the initial phase (t_1^0, t_2^0) of the modulation waves, as indicated in Table 2. The space groups in the conventional three-dimensional space of both structures, $P\bar{4}$ and $P2_12_12$, are the maximal non-isomorphic subgroups of the space group $P\bar{4}2_1m$ of the high-temperature phase, as indicated in International Tables for Crystallography (1989, Vol. A). $Cmm2$ is also one of the maximal non-isomorphic subgroups, but this is not allowed for $q = 1/3$, q with an odd denominator. The construction with $q = 1/3$ indicates that no mirror plane is in the structures.

The present method may be applicable to structural studies on the materials whose structures do not change in $(3 + d)$-dimensional spaces and the relative phase changes of the modulation waves are induced by deformation of the $(3 + d)$-dimensional cells.

References

Bindi, L., Bonazzi, P., Dusek, M., Petrícek, V. & Chapuis, G. (2001). Acta Cryst. B**57**, 739–746.

Bindi, L., Czank, M., Röthlisberger, F. & Bonazzi, P. (2001). Am. Mineral. **86**, 747–751.

Hagiya, K., Kusaka, K., Ohmasa, M. & Iishi, K. (2001). Acta Cryst. B**57**, 271–277.

Hagiya, K., Ohmasa, M. & Iishi, K. (1992). Proc. Jpn Acad. Ser. B, **68**, 25–29.

Hagiya, K., Ohmasa, M. & Iishi, K. (1993). Acta Cryst. B**49**, 172–179.

Hemingway, B. S., Evans, H. T. Jr, Nord, G. L. Jr, Haselton, H. T. Jr, Robie, R. A. & McGee, J. J. (1986). Can. Mineral. **24**, 425–434.

Heurck, C. van, Tendeloo, G. van & Amelinckx, S. (1992). Phys. Chem. Miner. **18**, 441–452.

Kusaka, K. (1999). PhD thesis, Himeji Institute of Technology, Japan.

Kusaka, K., Hagiya, K., Ohmasa, M., Okano, Y., Mukai, M., Iishi, K. & Haga, N. (2001). Phys. Chem. Miner. **28**, 150–166.

Kusaka, K., Ohmasa, M., Hagiya, K. & Iishi, K. (1998). Miner. J. **20**, 47–58.

Riester, M. & Böhm, H. (1997). Z. Kristallogr. **212**, 506–509.

Riester, M., Böhm, H. & Petrícek, V. (2000). Z. Kristallogr. **215**, 102–109.

Seifert, F., Czank, M., Simons, B. & Schmahl, W. (1987). Phys. Chem. Miner. **14**, 26–35.

Smaalen, S. van (1987). Acta Cryst. A**43**, 202–207.

Smyth, J. R. & Bish, D. L. (1988). Crystal Structures and Cation Sites of the Rock-Forming Minerals. Boston: Allen and Unwin.